Snowmelt detection over the Greenland ice sheet from SSM/I brightness temperature daily variations

Marco Tedesco[1,2]

Received 13 October 2006; revised 30 November 2006; accepted 19 December 2006; published 27 January 2007.

[1] We propose a technique for monitoring snowmelt over the Greenland ice sheet between 1992 and 2005 based on the difference between ascending and descending brightness temperatures (DAV) measured either at 19.35- or 37- GHz by the Special Sensor Microwave Imager (SSM/I). Wet snow is detected when both brightness temperatures and DAV values exceed fixed thresholds. Differently from existing techniques, a multi-frequency approach allows detection of wet snow at different depths and intensities, providing a tool for improving climatological and hydrological applications. Air temperature values either recorded by ground based stations or derived from model are used for calibrating and validating the technique. Results are compared with those obtained using backscattering coefficients recorded by the NASA's Quick Scatterometer (QuikSCAT) during an extreme melting event occurring on June 2002. Long-term results show that snowmelt extent has been increasing at a rate of ~40,000 Km^2 per year for the past 14 years. **Citation:** Tedesco, M. (2007), Snowmelt detection over the Greenland ice sheet from SSM/I brightness temperature daily variations, *Geophys. Res. Lett.*, *34*, L02504, doi:10.1029/2006GL028466.

1. Introduction and Background

[2] Monitoring the area extent and duration of superficial snowmelt in Greenland is important for multiple reasons. Differently from dry snow, wet snow has a relatively low albedo at visible and near-infrared spectral bands, absorbing more incoming solar radiation than dry snow. Moreover, *Abdalati and Steffen* [1997] observed that increased melt can provide a vapor source for cloud formation, which, in turn, will increase the down-welling longwave radiation. This implies that the instability of the ice sheet due to snowmelt may be much greater than the simple albedo effect.

[3] Microwave data are very sensitive to liquid water within the snowpack and represent a valuable tool for monitoring the long-term evolution of areal extent and duration of snowmelt because at the frequencies of interest (e.g., near 19 and 37 GHz), they do not depend on solar illumination and are only weakly affected by cloud presence.

[4] Several methods have been proposed in the literature for detecting melting snow from space-borne passive microwave data. For example, *Mote et al.* [1993] and *Zwally and Fiegles* [1994] proposed to use the difference between the daily 19 GHz brightness temperature and a mean brightness temperature: if the difference ($T_b - T_{mean}$) was greater than a fixed threshold then snow was classified as wet. *Steffen et al.* [1993] used the normalized gradient ratio GR = ($T_{b19H} - T_{b37H}$)/($T_{b19H} + T_{b37H}$) as a surface melt index, determining a wet snow threshold by comparing satellite data and in situ measurements. Later, *Abdalati and Steffen* [1995, 1997], replaced the horizontally polarized brightness temperature at 37 GHz with the vertical polarization, defining the cross-polarization gradient ratio XPGR = ($T_{b19H} - T_{b37V}$)/($T_{b19H} + T_{b37V}$). A different approach for detecting melting snow in Alaska was proposed by *Ramage and Isacks* [2002], which makes use of the difference between brightness temperatures collected during ascending and descending passes (diurnal amplitude variations = DAV). Melting onset and wet snow areas are identified according to the condition that both brightness temperature at 37 GHz and DAV values exceed fixed threshold values (being, respectively, 246 K and 10 K). Melt-onset timing was corroborated by *Ramage and Isacks* [2003] based on regional river discharge records for a period that overlapped satellite data.

[5] In this study, we apply, for the first time, a DAV-based technique for mapping the areal extent of melting snow in Greenland by using brightness temperatures at 19.35 GHz, horizontal polarization, or 37 GHz, vertical polarization, measured by the Special Sensor Microwave/Imager (SSM/I) radiometer. In contrast to the techniques proposed so far, the use of both ascending and descending passes enhances the sensitivity of the technique to the daily melting cycle. Moreover, the separate use of multiple frequencies permits the study of melting involving different depths and having different intensities. These last two points are major advantages of the DAV-based technique with respect to those proposed in the literature so far. Threshold values used in the original study by *Ramage and Isacks* [2002] are recomputed to account for the differences between the two areas (the original work was focused on Alaska) and for the new frequency. This is accomplished by using values of air temperature recorded by the Greenland Climate Network (GC-NET) [e.g., *Steffen et al.*, 1996] and surface temperature values obtained from NCEP/NCAR Reanalysis-1 data [*Kalnay et al.*, 1996]. Preliminary results of a comparative analysis between the results obtained here and those obtained using either the XPGR approach or another approach making use of backscattering coefficients measured by the NASA's Quick Scatterometer (QuikSCAT) are reported. An extreme melting event is identified at the end of June, 2002 and discussed. The temporal trend of daily areal extent of surface snowmelt for the period 1992–2005

[1] Goddard Earth Sciences and Technology Center, University of Maryland Baltimore County, Baltimore, Maryland, USA.
[2] Also at NASA Goddard Space Flight Center, Greenbelt, Maryland, USA.

0094-8276/07/2006GL028466$05.00

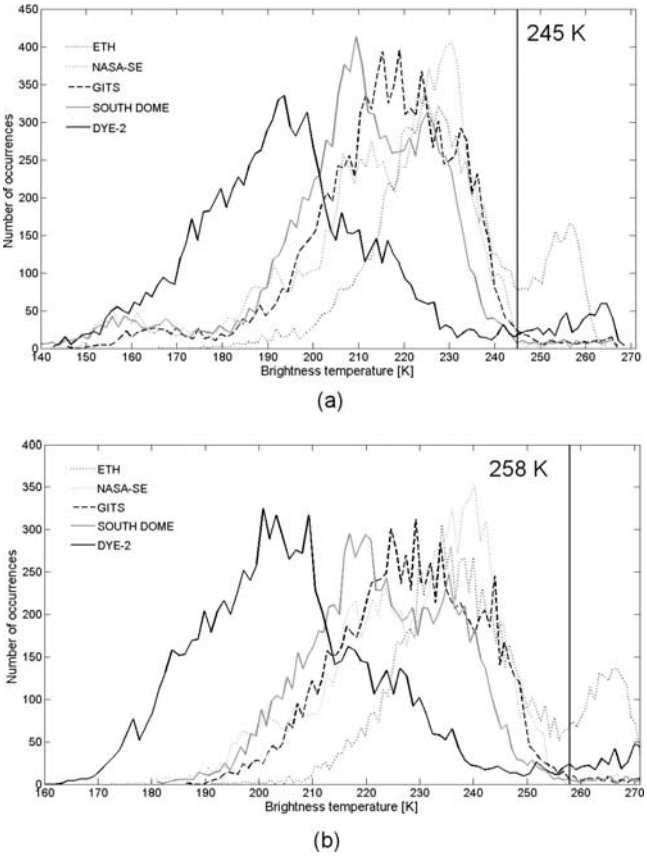

Figure 1. Histograms of ascending and descending SSM/I brightness temperatures at (a) 19.35 GHz (H pol.) and (b) 37 GHz (V pol.) 1992 through 2005 for the Swiss Camp (69.5732 N, 49.2952 E, black dotted line, the NASA-SE (66.4797N, 42.5002 E, gray dotted line), GITS (77.1433N, 61.0950 E, black line), SOUTH DOME (63.1489N, 44.8167 E, gray dashed line) and DYE-2 (66.4810 N, 46.2800 E, black dashed line) GCNET stations. Vertical line represents Tb melt threshold used in this study. Data are from F11 and F13 SSM/I satellites.

is reported together with the total extent of snowmelt for each year and the relative trend.

2. The Diurnal Amplitude Variation (DAV) Technique Over Greenland

[6] A strong and sudden increase of the imaginary part of snow permittivity and brightness temperature occurs when liquid water particles appear within the snowpack [e.g., *Tedesco et al.*, 2006], even in small amount. As a consequence, if, for example, snow is dry during the night (either frozen or refrozen) and it becomes wet during the day, then daytime brightness temperature will be much higher than that acquired during the nighttime. Also, if melting persists during the night then brightness temperature will remain high. Increases in brightness temperature can be also caused by other factors such as a decrease of effective grain size due to new snow or changes in snow temperature [e.g., *Tedesco et al.*, 2006]. However, these processes are not as sudden and strong as the appearance of liquid water within the snowpack within a diurnal cycle.

[7] The approach used here is based on the one proposed by *Ramage and Isacks* [2002], who were the first to suggest that the technique could be also applied to Greenland [*Ramage*, 2001; *Ramage and Isacks*, 2003]. Here we extend the technique also to the 19.35 GHz channel and use it, for the first time, over the Greenland ice sheet. Wet snow is detected when 1) the brightness temperature (37 GHz, vertical polarization, or 19.35 GHz, horizontal polarization) and 2) the difference between ascending and descending passes exceed fixed threshold values ($Tb > A$ and $DAV = abs(Tb_{ascending} - Tb_{descending}) > B$, where A and B are threshold values to be determined). In order to account for melting that eventually might persist during the night we also introduce the rule that snow is melting when both ascending and descending brightness temperatures are greater than the threshold value A. We use SSM/I Level 3 Equal-Area Scalable Earth-Grid (EASE-Grid) brightness temperatures (*Armstrong et al.* [1994], updated through 2005) collected onboard the F11 (1992–1995) and F13 (1995–2005) satellites gridded to 25 km resolution (http://www.nsidc.org/data/docs/daac/nsidc0032_ssmi_ease_tbs.gd.html). Data here used were collected between ~17:00 (5:00) and ~18:30 (6:30) local time during the ascending (descending) pass.

[8] We derive the threshold value (A) using the histograms of brightness temperatures [*Ramage*, 2001; *Ramage and Isacks*, 2003] collected over those areas including the pixels containing the 20 GCNET stations during the period January 1, 1992–December 31, 2005. As an example, Figure 1 shows the histograms of brightness temperatures at 19.35 GHz, horizontal polarization (Figure 1a) and 37 GHz, vertical polarization (Figure 1b), both ascending and descending passes for the EASE-grid pixels containing the Swiss Camp (Lat. 69.5732 N, Lon. 49.2952 E, black dotted line), the NASA-SE (Lat. 66.4797 N, Lon. 42.5002 E, gray dotted line), the GITS (Lat. 77.1433 N, Lon. 61.0950 E, black line), the SOUTH DOME (Lat. 63.1489N, Lon. 44.8167 E, gray dashed line) and the DYE-2 (Lat. 66.4810 N, Lon. 46.2800 E, black dashed line) GCNET stations. The histograms can be modeled by means of a bimodal distribution, with the separation between wet and dry snow cases being apparent at both frequencies and for all test sites. A comparative analysis carried out over the 20 GCNET test sites (not reported here for reasons of brevity) leads us to threshold values of $A = 245\ K$ for the 19.35 GHz and $A = 258$ K for the 37 GHz channels (being 246 K in the work by *Ramage and Isacks* [2002]). We observe from Figure 1 that the threshold value is close to the right peak of the two curves of the bimodal distribution for all cases and frequencies reported, suggesting that the selected threshold can be assumed to be valid at different locations and for the climate/snow condition gradients they represent. The threshold value (B) on the DAV is determined using air temperature values collected by the GCNET stations and National Centers for Environmental Prediction/National Center for Atmospheric Research (NCEP/NCAR) daily mean surface temperature values. We use both data sets because GCNET air temperature is collected at high temporal resolution but only at a point scale and in some specific locations while the NCEP/NCAR reanalysis surface temperature has a low temporal resolution but is spatially well-distributed. Generally, to determine if snow is melting it is necessary to know the surface energy balance terms, namely net short-wave and

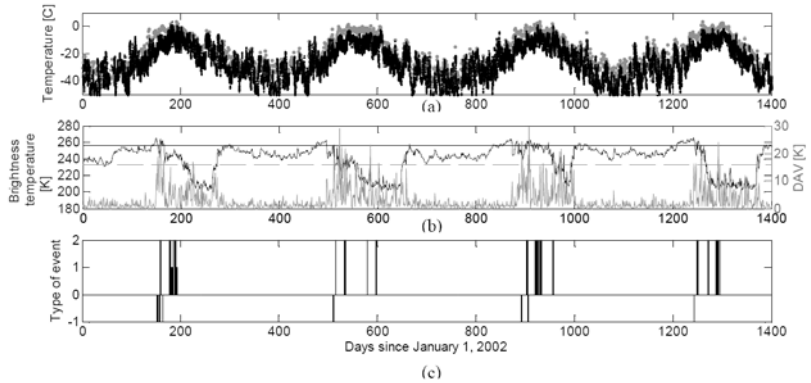

Figure 2. Temporal behavior of (a) air temperatures recorded by the GCNET station (gray dots) and obtained from NCEP/NCAR reanalysis (black squares), (b) both brightness temperature at 37 GHz, vertical polarization (black line, left axis) and DAV (gray line, right axis), together with the threshold values of 258 K (continuous horizontal line) and 18 K (dashed horizontal line), and (c) type of event occurring for the pixel containing the NASA-E GCNET station. Here, event = 1 means melting assumed according to GCNET air temperature values, event = 2 melting assumed according to the NCEP/NCAR air temperature values and event = −1 melting detected according to the microwave-based technique.

long-wave radiation fluxes, and sensible, latent-heat and conductive-heat fluxes. However, in this study we use air temperature as an indicator of melting and assume that melting can occur when air temperature exceeds 0 ° [*Nghiem et al.*, 2001; *Steffen and Box*, 2001; *Steffen et al.*, 2004]. The value selected for B at 19.35 GHz is 25 K and 18 K at 37 GHz. Also in this case we paid attention not to overestimate the extent of melting areas, by minimizing the number of cases when the algorithm was detecting melting but the air temperature analysis was not.

[9] As an example, we report in Figure 2 air temperature recorded by the GCNET station (gray dots) and surface temperature obtained from NCEP/NCAR data (black squares) (Figure 2a), brightness temperature at 37 GHz, vertical polarization (black line, left axis) and DAV (gray line, right axis) with the horizontal lines representing the threshold values on the brightness temperature (258 K, continuous horizontal line) and on DAV (18 K, dashed horizontal line) (Figure 2b) and type of event occurring for the pixel containing the station NASA-E of the GCNET (Lat. 75 N, Lon. 29.9997 E) (Figure 2c). Here event = 1 corresponds to melting detected when GCNET air temperature values exceeds 0° C, event = 2 to melting detected when NCEP/NCAR surface temperature exceeds 0° C and, finally, event = −1 to melting detected with the DAV-based technique. Graphically, positive bars mean melting estimated from air/surface temperature values where negative ones mean melting detected by the DAV-based technique. In this particular case, the DAV-based technique is capable of matching melting estimated from the analysis of air/surface temperature when melting has started occurring. Although the technique is not able to match all melting events identified by the analysis of air temperature, we observe that generally it is not detecting melting when it is not happening, hence not overestimating the number of events when wet snow is present.

3. Results and Discussion

[10] Validation of the proposed approach is not an easy task for several reasons. First, the limited number of ground measurements and the remoteness of the area under study are strong limiting factors. Second, existing measurements are collected at point scale and are compared with retrievals performed at 25 km resolution. This is a common problem in remote sensing and can lead to large errors. Last, measurements of snow wetness are affected by high uncertainty, making the comparison between measured and derived values more difficult. We strongly suggest that concurrent measurements of microwave radiometric data and snow properties will be performed to generate a reliable data set for the validation of the proposed techniques. In the meantime we propose a cross-validation approach for evaluating the performance and the reliability of the DAV technique here proposed. We compare the results obtained with the DAV-based technique with those 1) obtained either using the XPGR approach [e.g., *Abdalati and Steffen*, 1997] and another approach based on diurnal variations of backscattering coefficients measured by QuickSCAT [*Nghiem et al.*, 2001] for a specific period in 2002 and 2) using both XPGR and NCEP/NCAR surface temperature analysis for the period 1992–2005.

[11] We identified an extreme melting event from June 27 to July 1, 2002, as noticeable from NCEP/NCAR reanalysis mean daily surface temperature exceeding 0 ° C for a large part of the Greenland surface (Figure 3a). Figure 3b shows the maps derived from the XPGR approach (SSM/I); Figures 3c and 3d show the areal extent of snow melt detected with the DAV-based technique for the same dates using, respectively, the 19.35- (Figure 3c) and 37 - GHz (Figure 3d); Figure 3e shows the maps derived from QuikSCAT data. First we observe that, as expected [e.g., *Steffen et al.*, 2004], the techniques based on passive data (XPGR and DAV) are less sensitive than the one based on active measurements (QuikSCAT), which predicts approximately 30 % more areal extent than the passive approaches. Then we observe that both 19.35 and 37 GHz DAV- and QuikSCAT-based approaches provide maps of melting area that are spatially consistent with the distribution of surface temperature. On June 27, 2002 the surface temperature (Figure 3a) is above 0° C for those areas with latitude around 70° N. Areas above this latitude are below 0° C,

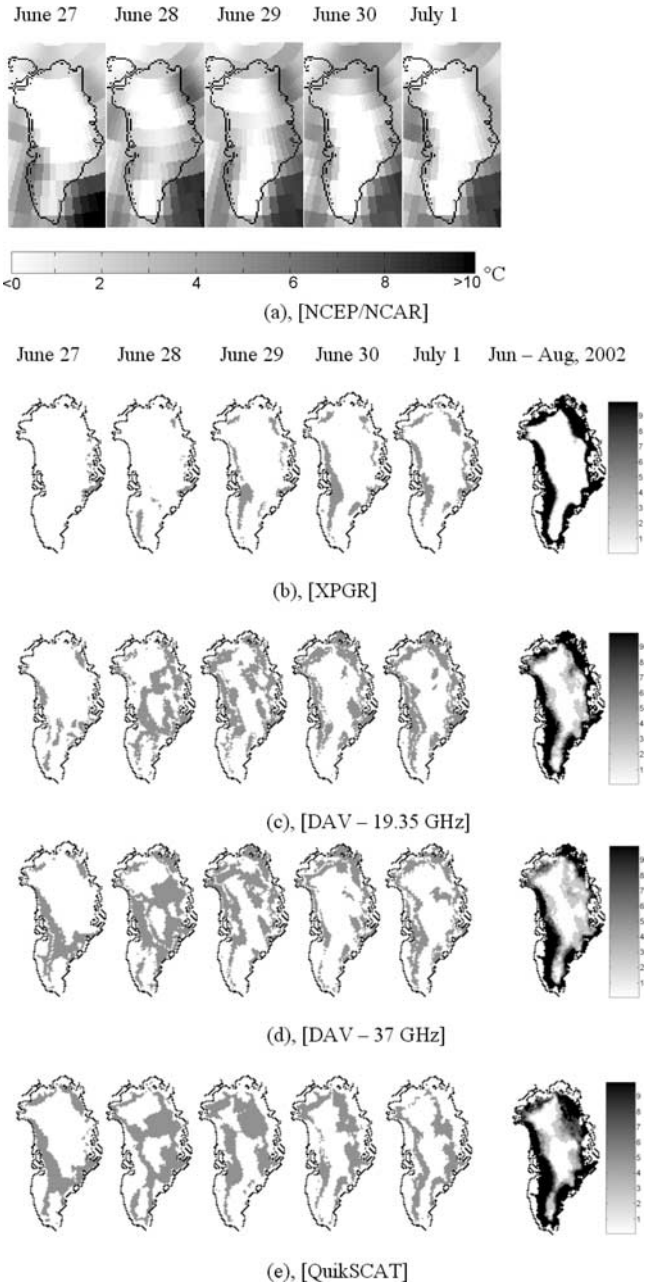

Figure 3. Comparison between (a) NCEP/NCAR near surface daily temperatures for the period June, 27 – July 1, 2002, areal extent of surface snow melt derived from (b) the XPGR-based technique and (c) the technique proposed in this study using brightness temperatures at 19.35 GHz. (d) Same as Figure 3b but at 37 GHz and (e) QuikSCAT data. The areal extent and the total number of days for the period June 1, 2002 – August 31, 2002 is also shown on the right.

with the exception of the low altitude coastal areas. We see that the corresponding maps derived from active and DAV-based approach show melting below 70 °N and along the west coast of Greenland and are consistent with the surface temperature distribution. In this case the agreement between DAV- and QuikSCAT-based approaches is around 60 % for the 37 GHz and 45 % for the 19.35 GHz. On June 28 and June 29, 2002 high altitude areas with latitude lower than 65 ° N and around 75 °N have a temperature below 0 °C but temperatures are equal to or greater than 0 °C over the remaining part of Greenland surface. Also in this case, maps of snowmelt areal extent derived with the active and DAV-based techniques are in agreement with the spatial distribution of surface temperature. Results show that the XPGR technique is not sensitive to melting observed on June 27 and 28, 2002. This might be due to the fact that, as brightness temperatures at 19.35 GHz have a higher penetration depth and are less sensitive to wetness than those at 37 GHz [e.g., *Tedesco et al.*, 2006], a technique based on both channels requires higher values of snow wetness than one based on only the 37 GHz channel. Also, the choice of using daily average brightness temperature values is responsible for the sensitivity of the XPGR algorithm. On June 30 and July 1, 2002 surface temperature in the interior of Greenland goes below 0 °C again, while the areas close to the coast are still above 0 ° C. Again, maps of snowmelt extent derived with the DAV approach and QuikSCAT are in agreement with this scenario. In these cases, the XPGR approach is sensitive to melting events along the coast, but it is insensitive to the melting in the interior of Greenland. In Figure 3, as a reference, the maps on the right of Figure 3 reproduce the areal extent of surface snowmelt and the total number of days derived for the period June–August 2002 from the different remote sensing techniques.

[12] Figure 4 shows the daily area extent of surface snow melt (gray line) and total melt area extent (TES, e.g. the extent of area experiencing at least one day of melting, black solid line), in million of km^2, for the period 1992–2005 derived with the XPGR – based approach (Figure 4a), analysis of NCEP/NCAR surface temperatures (e.g., melting occurring when surface temperature is greater than or equals to 0°C) (Figure 4b), DAV-based technique using the 19.35 GHz brightness temperatures (Figure 4c) and DAV – based technique using the 37 GHz brightness temperatures (Figure 4d). The dashed lines represent the linear fit to the total area extent. First, we note that all techniques show consistently a positive trend in the increase of the TES from 1992 to 2005. To our knowledge, this is the first time that results obtained with different techniques and approaches are compared to evaluate the trend of TES. We computed the regression coefficient and the coefficient of determination between the TES derived from the analysis of NCEP/NCAR surface temperature and the remaining techniques. The computed correlation coefficients (r) and coefficient of determination (R^2) are r = 1.44 and R^2 = 0.83 in the case of XPGR, r = 1.20 and R^2 = 0.84 in the case of DAV – 19 GHz and r = 1.12 and R^2 = 0.82 in the case of DAV – 37 GHz. It follows that, although all techniques show a similar trend, results obtained with DAV – based techniques making use of the 19.35 – and 37 – GHz are in better agreement with those from the analysis of the NCEP/NCAR surface temperatures than those obtained with the XPGR approach. This suggests that the DAV approach might be able to catch features that the XPGR cannot.

[13] A more detailed analysis of the daily values obtained with the DAV techniques shows that early surface melting events can be observed using the 37 GHz-based approach in 1998 (April 9) and 2000 (April 12) although the area involved is small (~40,000 Km^2). Also, late melting events

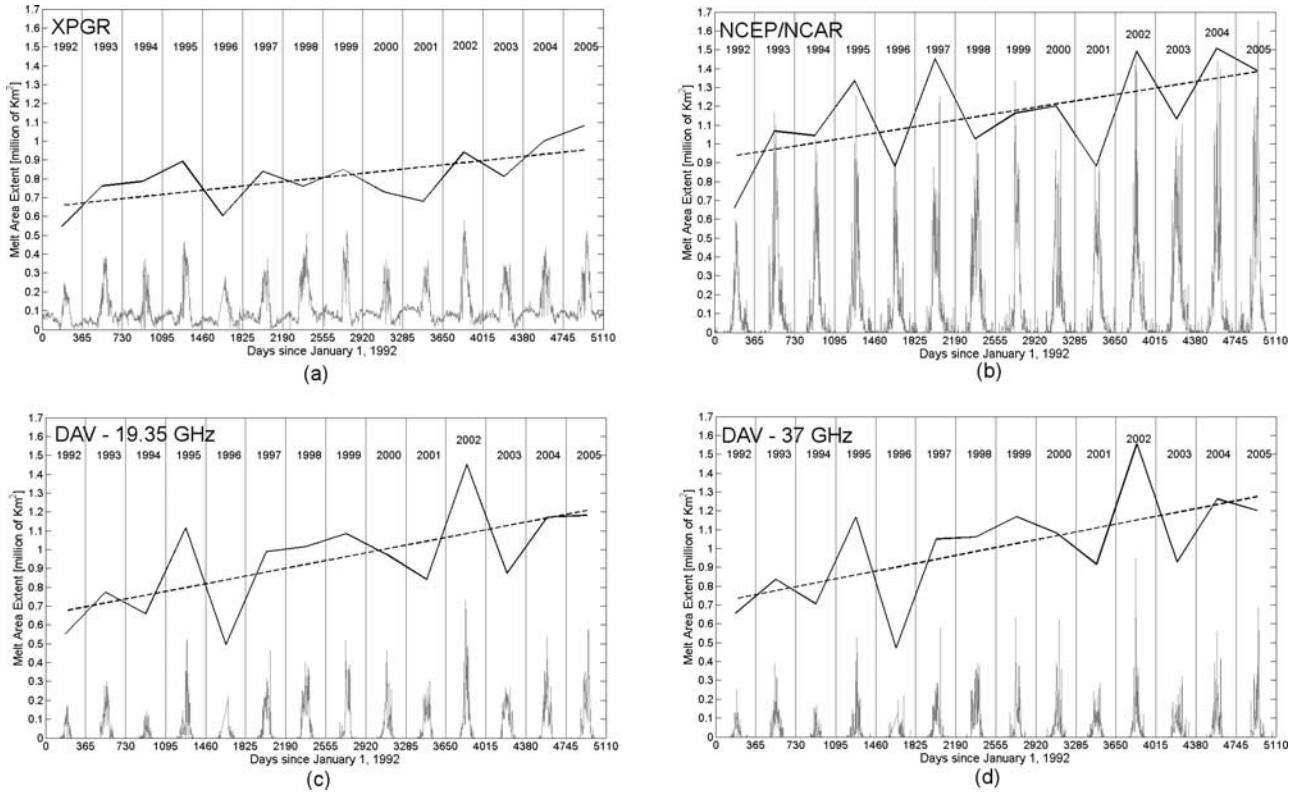

Figure 4. Daily areal extent of surface snow melt and total area extent (in million of km^2) for the period 1992 –2005 derived with the (a) XPGR – based approach, (b) NCEP/NCAR surface temperatures and (c) DAV-based technique using the 19. 35 GHz brightness temperatures and (d) Same as Figure 4c but at 37 GHz. Dashed lines represent the linear fit to the total area extent.

occur in 1995 (November 8) and 1996 (November 12), with an area of approximately 30,000 Km^2. We observe low values of daily melting extent areas from both 19.35- and 37- GHz DAV-based approaches in 1992, 1993, 2001 and 2003. The greatest daily value occurred at the end of June, 2005, with an area of approximately 750,000 Km^2 (19.35 GHz) and 950,000 Km^2 (37 GHz) (see Figure 3). The lowest TES value is observed in 1992, with, respectively, 553,125 Km^2 (19.35 GHz) and 656,875 Km^2 (37 GHz), closely followed by year 1994 with 659,375 Km^2 (19.35 GHz) and 705,625 Km^2 (37 GHz). The highest value for TES is observed in 2002, with 1,451,875 Km^2 (19.35 GHz) and 1,555,625 Km^2 (37 GHz), corresponding to ~90 % (37 GHz) and ~85 % (19 GHz) of the entire Greenland ice sheet surface. A linear trend fit of the TES values suggests that the areal extent experiencing at least one day of melting has been increasing since 1992 at an average rate of 40,924 Km^2 per year as derived from the 19.35 GHz channel and 41,573 Km^2 per year as derived from the 37 GHz channel, corresponding, respectively, to 2.33 % (19.35 GHz) and 2.37 % (37 GHz) of the entire ice sheet surface.

4. Conclusions and Future Work

[14] SSM/I brightness temperatures either at 19.35 or 37 GHz acquired during ascending and descending passes have been used, for the first time, for mapping the surface snowmelt over Greenland. For a given frequency, when both brightness temperature and the difference between the values collected during ascending and descending passes exceed fixed thresholds then snow is classified as wet. Threshold values have been re-computed with respect to those reported in the literature and have been fixed to 245 K (19.35 GHz) and 258 K (37 GHz) for the brightness temperatures and 25 K (19.35 GHz) and 18 K (37 GHz) for the DAV (SSM/I). They were derived from the analysis of histograms of brightness temperatures for different years over several locations and through a comparative analysis between air/surface temperature and microwave radiometric data. There are two major advantages in the technique proposed here with respect to those existing in the literature: 1) the use of both ascending and descending passes increases the sensitivity to daily variability melting cycle with respect to the use of daily average brightness temperatures; 2) the use of multiple frequencies allows to study melting at different depths and with different intensities. A first step toward the validation/calibration of the proposed approach was made by comparing the areal extent of snowmelt derived from QuikSCAT backscattering coefficients and both DAV- and XPGR-based when an extreme melting event was occurring in 2002. As expected, QuikSCAT was found to be more sensitive to the presence of liquid water. Results also showed that results derived with the two techniques (active and passive) making use of diurnal variations are consistent with each other. Furthermore, these results appeared to be consistent with the distribution of

surface temperature derived from NCEP/NCAR reanalysis data.

[15] The analysis of daily melt areal extent between 1992 and 2005 helped us to identify early (1998, 2000) and late (1995, 1996) melting events, involving areas between 30,000 and 40,000 Km^2. The maximum daily areal extent was recorded on June 27, 2002 with a value of 750,000 Km^2 (19.35 GHz) and 950,000 Km^2 (37 GHz). We also reported the areal extent of those areas experiencing at least one day of melting (named TES, Figure 4, black thick lines). In this case the smallest value is obtained in 1992 with 553,125 Km^2 (19.35 GHz) and 656,875 Km^2 (37 GHz), where the highest is obtained in 2002, with 1,451,875 Km^2 (19.35 GHz) and 1,555,625 Km^2 (37 GHz). This corresponds to over ~85 % (19.35 GHz) and ~90 % (37 GHz) of the entire Greenland ice sheet surface. Results obtained with the DAV approach were compared with those obtained from XPGR and NCEP/NCAR surface temperature. To our knowledge, this is the first time that results using independent techniques and independent datasets are compared. Results show that all techniques agree that there is a positive trend in the increase of the area experiencing at least one day of melting from years 1992 through 2005. However, the rate at which this increase is occurring changes depending on the approach used. Results obtained with the DAV approach suggested that the areal extent experiencing at least one day of melting has been increasing since 1992 at a rate of 40,924 Km^2 per year (19.35 GHz, surface or deeper layers) and 41,573 Km^2 (37 GHz, surface melting), corresponding to ~ 2.3 % of the entire Greenland surface ice sheet.

[16] Further validation of the proposed technique is already in progress, together with the improvement of the determination of threshold coefficients through a multilayer electromagnetic model and the inter-comparison of daily derived areal extent maps from both active and passive microwave instruments. A comparative analysis of concurrent observations of snow albedo (e.g., GCNET or MODIS) and radiometric data is already in progress to study the correlation between the melting detected using microwaves and the changes in the albedo due to surface changes (e.g., grain size increase after melting). However, field experiments performing concurrent measurements of microwave radiometric data and snow properties are mandatory to provide a reliable (and lacking) validation data set. Future work will include the application of the proposed technique to F08-SSM/I and AMSR-E brightness temperatures.

[17] **Acknowledgments.** Joan Ramage is deeply acknowledged for the useful and fundamental discussions about the DAV method. Thanks to Konrad Steffen, Kyle McDonald and Jeff Miller for providing, respectively, GCNET, QuikSCAT and NCEP/NCAR data. Also thanks to Chris Shuman and Waleed Abdalati for the constructive discussions.

References

Abdalati, W., and K. Steffen (1995), Passive microwave-derived snow melt regions on the Greenland ice sheet, *Geophys. Res. Lett.*, *22*, 787–790.

Abdalati, W., and K. Steffen (1997), Snowmelt on the Greenland ice sheet as derived from passive microwave satellite data, *J. Clim.*, *10*, 165–175.

Armstrong, R. L., K. W. Knowles, M. J. Brodzik, and M. A. Hardman (1994), DMSP SSM/I Pathfinder daily EASE-grid brightness temperatures, 1992–2005, digital media, Natl. Snow and Ice Data Cent., Boulder, Colo.

Kalnay, E., et al. (1996), The NCEP/NCAR 40-year reanalysis project, *Bull. Am. Meteorol. Soc.*, *77*, 437–470.

Mote, T. L., M. R. Anderson, K. C. Kuivenen, and C. M. Rowe (1993), Passive microwave derived spatial and temporal variations of summer melt on Greenland ice sheet, *Ann. Glaciol.*, *17*, 233–238.

Nghiem, S. V., K. Steffen, R. Kwok, and W.-Y. Tsai (2001), Detection of snowmelt region on the Greenland ice sheet using diurnal backscatter change, *J. Glaciol.*, *47*, 539–547.

Ramage, J. M. (2001), Satellite remote sensing of daily, seasonal, and annual changes on southeast Alaskan glaciers 1986–1998, Ph.D. dissertation, Cornell Univ., Ithaca, N. Y.

Ramage, J. M., and B. L. Isacks (2002), Determination of melt-onset and refreeze timing on southeast Alaskan icefields using SSM/I diurnal amplitude variations, *Ann. Glaciol.*, *34*, 391–398.

Ramage, J. M., and B. L. Isacks (2003), Interannual variations of snowmelt and refreeze timing in southeast Alaskan iceshields using SSM/I diurnal amplitude variations, *J. Glaciol.*, *49*, 102–116.

Steffen, K., and J. E. Box (2001), Surface climatology of the Greenland ice sheet: Greenland Climate Network 1995–1999, *J. Geophys. Res.*, *106*, 33,951–33,964.

Steffen, K., W. Abdalati, and J. Stroeve (1993), Climate sensitivity studies of the Greenland ice sheet using AVHRR, SMMR, SSM/I and in situ data, *Meteorol. Atmos. Phys.*, *51*, 239–258.

Steffen, K., J. E. Box, and W. Abdalati (1996), Greenland Climate Network: GC-Net, in *Special Report on Glaciers, Ice Sheets and Volcanoes, Tribute to M. Meier, CRREL 96-27*, edited by S. C. Colbeck, pp. 98–103, Cold Reg. Res. and Dev. Cent., Hanover, N. H.

Steffen, K., S. V. Nghiem, R. Huff, and G. Neumann (2004), The melt anomaly of 2002 on the Greenland ice sheet from active and passive microwave satellite observations, *Geophys. Res. Lett.*, *31*, L20402, doi:10.1029/2004GL020444.

Tedesco, M., E. J. Kim, A. W. England, R. de Roo, and J. P. Hardy (2006), Brightness temperatures of snow melting/refreezing cycles: Observations and modeling using a multilayer dense medium theory-based model, *IEEE Trans. Geosci. Remote Sens.*, *44*(12), 3563–3573.

Zwally, H. J., and S. Fiegles (1994), Extent and duration of Antarctic surface melting, *J. Glaciol.*, *40*, 463–476.

M. Tedesco, Goddard Earth Sciences and Technology Center, University of Maryland Baltimore County, 5523 Research Park Drive, Suite 320, Baltimore, MD 21228, USA. (mtedesco@umbc.edu)